Isolated versus Condensed Anion Structure III: The Influence of the Cations 1,3-propanediammonium, 1,4-butanediammonium, *n*-propylammonium, *n*-butylammonium and *n*-pentylammonium on Structures and Phase Transitions of $ZnBr_4^{2-}$ Salts. A ^{81}Br NQR and X-ray Structure Analysis

Hideta Ishihara[a], Shi-qi Dou, Keizo Horiuchi[b], Helmut Paulus, Hartmut Fuess, and Alarich Weiss†

Fachbereich Materialwissenschaft, Fachgebiet Strukturforschung,
Technische Hochschule Darmstadt, Petersenstraße 23, D-64287 Darmstadt, Germany
[a] Faculty of Culture and Education, Saga University, Honjo-machi 1, Saga 840, Japan
[b] College of Science, University of the Ryukyus, 1 Senbaru, Nishihara, Okinawa 903-01, Japan

Z. Naturforsch. **52a**, 550–560 (1997); received March 12, 1997

The influence of the cations on the condensation of the anions in the salts (A′)Zn(II)Br_4 and $(A)_2$Zn(II)Br_4 is studied by ^{81}Br NQR and X-ray crystal structure analysis. (A′)Zn(II)Br_4(A′ = $[H_3N(CH_2)_3NH_3]^{2+}$) (**1**) shows a phase transition at 474 K. The phase II of (**1**) crystallizes with isolated $[ZnBr_4]^{2-}$ tetrahedra: monoclinic $P2_1/n$, Z = 4, $a = 1108.4(5)$, $b = 1096.8(2)$, $c = 1118.5(6)$ pm, and $\beta = 117.07(4)°$ at 296 K. A quartet was observed in the ^{81}Br NQR spectrum of phase II: 61.634, 58.062, 56.675, and 53.673 MHz (77 K); 59.193, 57.448, 56.015, and 52.515 MHz (301 K). $(A)_2ZnBr_4$(A = $[n\text{-}H_3C(CH_2)_2NH_3]^+$ (**2**) and $[n\text{-}H_3C(CH_2)_3NH_3]^+$ (**3**)) also show structures with isolated $[ZnBr_4]^{2-}$ tetrahedra. The compound (**2**) crystallizes with $P2_1/c$, Z = 4, $a = 771.8(3)$, $b = 1061.9(4)$, $c = 2054.2(7)$ pm, and $\beta = 106.75(1)°$ at 291 K. The compound (**3**) crystallizes with $P2_1/c$, Z = 4, $a = 768.9(4)$, $b = 2229.6(10)$, $c = 1071.6(5)$ pm, and $\beta = 91.70(3)°$ at 295 K. ^{81}Br NQR and DSC measurements on $[H_3N(CH_2)_4NH_3]ZnBr_4$ (**4**), and $[n\text{-}H_3C(CH_2)_4NH_3]_2ZnBr_4$ (**5**) were also performed. The compound (**4**) shows several phase transitions at 349 K and higher temperatures, and a quartet in the ^{81}Br NQR spectrum could be observed between 77 and 330 K: 65.992, 65.544, 59.900, and 50.162 MHz (77 K); 63.787, 62.963, 59.928, and 50.364 MHz (320 K). The compound (**5**) shows also a phase transition at 244 K, and a quartet of ^{81}Br lines could be observed in the NQR spectrum between 77 and 244 K: 61.279, 58.933, 57.869, and 56.485 MHz (77 K); 59.712, 56.936, 57.409, and 54.793 MHz (240 K). The various influences of the cations, such as size and hydrogen bonds on the condensation of $[MX_4]^{2-}$ (M = Zn, Cd; X = Cl, Br) are discussed.

Introduction

In the recent studies of complex salts with bromocadmate anions $[CdBr_{2+n}]^{n-}$ by X-ray diffraction and ^{79,81}Br NQR a variety of polymer anionic structure types [1–5] and of isolated $[CdBr_4]^{2-}$ tetrahedra [6] were determined. The compounds $[H_3N(CH_2)_3NH_3]CdBr_4$ [7, 8] and $[n\text{-}H_3C(CH_2)_2NH_3]_2CdBr_4$ [8] crystallize in perovskite-type layer structures of the anions and exhibit phase transitions due to the dynamics of the NH_3^+ groups and the rotational motion of the alkyl chains about their long axes. In these investigations we have discussed the influence of the cation size, hydrogen bond, and bridging power of halogen atoms on the condensation of $[CdX_4]^{2-}$. Moreover, we have observed phase transitions in bis(alkylammonium) tetrabromozincate(II) [9]. In the following we report on the crystal structure of $[H_3N(CH_2)_3NH_3]ZnBr_4$ (**1**), $[n\text{-}H_3C(CH_2)_2NH_3]_2ZnBr_4$ (**2**), and $[n\text{-}H_3C(CH_2)_3NH_3]_2ZnBr_4$ (**3**) and the results of ^{81}Br NQR of (**1**), $[H_3N(CH_2)_4NH_3]ZnBr_4$ (**4**) and $[n\text{-}H_3C(CH_2)_4NH_3]_2ZnBr_4$ (**5**), and we compare their properties with those of $(A)_2CdBr_4$ and (A′)$CdBr_4$.

Experimental

The title compounds were synthesized from commercial amines (Aldrich), $ZnBr_2$, and HBr following [9]. The solutions of the compounds were evaporated in air at pH = 3. Small single crystals for the X-ray diffraction experiments were grown from aqueous solutions. The structures were determined using four circle X-ray diffractometers ((**1**): Enraf Nonius CAD4, (**2** and **3**): Stoe-Stadi-4). From the measured intensi-

---

Reprint requests to Prof. Hideta Ishihara.
† deceased.

0932-0784 / 97 / 0600-0550 $ 06.00 © – Verlag der Zeitschrift für Naturforschung, D-72027 Tübingen

ties, corrected for Lorentz-polarization and absorption effects, the structures were solved by direct methods, Fourier synthesis, and least squares analysis with the programs given in [10]. The ^{81}Br NQR spectra were recorded by an NQR spectrometer working in the superregenerative mode. The sample temperature was measured with a copperconstantan thermocouple, and the frequencies were determined by counting techniques. DSC was carried out above 130 K with a differential scanning calorimeter DSC220 from Seiko Instruments Inc. under the following conditions: sample weight ca. 10 mg, heating rate 2–10 K min^{-1} with flowing dry N_2 gas at 40 ml min^{-1}.

Results

Crystal Structures:

$[H_3N(CH_2)_3NH_3]ZnBr_4$ (1)

1,3-propanediammonium tetrabromozincate(II) (1) crystallizes at room temperature monoclinic with C_{2h}^5-$P2_1/n$; the lattice constants etc. are presented in Table 1 [11]. Table 2 lists the positional coordinates and isotropic displacement parameters, U_{eq}. Intramolecular distances and angles of the anions are given in Table 3. In Fig. 1 the formula unit is drawn with the numbering of the atoms and the thermal ellipsoids. Figure 2 shows the projection of the unit cell along [100] onto the *bc* plane. The $[ZnBr_4]^{2-}$ anion forms an isolated tetrahedron in (1) with small differences in the zinc–bromine distances, $238.9 \leq d(\mathrm{Zn-Br})/\mathrm{pm} \leq 241.7$ (mean value 240.5 pm), and the angles in the tetrahedron deviate only slightly from the mean value 109.4°, ranging from 106.2° to 112.1°. There is no symmetry center within the 1,3-propanediammonium cation in (1). Intramolecular distances and angles in the cations are listed in Table 4. The distances d(N–C) are 146.3 and 148.6 pm, and d(C–C) 149.8 and 150.4 pm. In Table 3 distances and angles of the N–H···Br hydrogen bonds in (1) are listed in consideration of the van der Waals radii of the NH_4^+ group and the Br atom,

Table 1. Experimental conditions for the crystal structure determinations and crystallographic data of 1,3-propanediammonium tetrabromozincate(II), $[H_3N(CH_2)_3NH_3]ZnBr_4$ (1), *n*-propylammonium tetrabromozincate(II), $[n\text{-}H_3C(CH_2)_2NH_3]ZnBr_4$ (2) *n*-butylammonium tetrabromozincate(II), $[n\text{-}H_3C(CH_2)_3NH_3]ZnBr_4$ (3). Diffractometer: Stoe-Stadi-4 (2 and 3), Enraf Nonius CAD4 (1); wavelength: 71.069 pm (MoKα); Monochromator: Graphite (002); scan $\omega/2\theta = 1/1$

Compound		(1)	(2)	(3)
Empirical formula		$C_3H_{12}Br_4N_2Zn$	$C_6H_{20}Br_4N_2Zn$	$C_8H_{24}Br_4N_2Zn$
Formula weight		461.15	505.24	533.30
Crystal size/(mm)^3		0.7 × 0.2 × 0.15	1.5 × 0.2 × 0.1	0.9 × 0.35 × 0.25
Temperature/K		296(2)	291(2)	295(2)
Absorption coeff./m^{-1}		14880	11180	9818
θ-range for data collected		$2.14 \leq \theta/° \leq 22.98$	$2.07 \leq \theta/° \leq 22.52$	$1.83 \leq \theta/° \leq 22.56$
Index ranges		$-12 \leq h \leq 11$, $0 \leq k \leq 12$, $-10 \leq l \leq 12$	$0 \leq h \leq 8$, $-11 \leq k \leq 2$, $-22 \leq l \leq 21$	$0 \leq h \leq 8$, $-24 \leq k \leq 5$, $-11 \leq l \leq 11$
Lattice constants				
a/pm		1108.4 (5)	771.8 (3)	768.9 (4)
b/pm		1096.8 (2)	1061.9 (4)	2229.6(10)
c/pm		1118.5 (6)	2054.2 (7)	1071.6 (5)
β/°		117.07(4)	106.75(1)	91.70(3)
$V \cdot 10^{-6}$/(pm)^3		1210.8 (9)	1612.1(16)	1836.3(26)
Space group		C_{2h}^5–$P2_1/n$	C_{2h}^5–$P2_1/c$	C_{2h}^5–$P2_1/c$
Formula units *Z*		4	4	4
ϱ_{calc}/Mg · m^{-3})		2.530(2)	2.081(2)	1.928(2)
F (000)		856	960	1024
Reflections collected		1882	4164	3465
Symmetry independent		1676	2121	2406
[R_{int}]			0.0275	0.0482
Data used		1676	2118	2394
Restraints/Parameters		0/92	2/123	8/141
Goodness of fit on F^2		0.900	1.083	1.042
Final $R(I > 2\sigma(I))$	R_1	0.0360	0.0407	0.0723
	wR_2	0.0992	0.0991	0.1850
R (all data)	R_1	0.0498	0.0545	0.1068
	wR_2	0.1084	0.1129	0.2342
Largest diff: (peak/hole)/(10^{-6} e(pm)^3)		0.933/−0.586	0.706/−0.530	1.547/−1.034
Max. and Min. Trans.			0.1083/0.3353	0.0521/0.1305
Extinction Coeff.		0.0519(7)	0.0037(4)	0.0031(7)
Point positions:		All atoms in 4e	All atoms in 4e	All atoms in 4e

Table 2. Atomic coordinates ($\times 10^4$) and isotropic parameters U_{eq} (in pm^2) for $[H_3N(CH_2)_3NH_3]ZnBr_4$ (**1**), $[n\text{-}H_3C(CH_2)_2NH_3]_2ZnBr_4$ (**2**), and $[n\text{-}H_3C(CH_2)_3NH_3]_2ZnBr_4$ (**3**). U_{eq} is defined as one third of the trace of the orthogonalized tensor U_{ij} [11] which has the form: $T = \exp\{-2\pi(U_{11}h^2a^{*2} + U_{22}k^2b^{*2} + U_{33}l^2c^{*2} + 2U_{12}hka^*b^* + 2U_{13}hla^*c^* + 2U_{23}klb^*c^*)\}$. The coordinates of the hydrogen atoms have been fixed in the least squares refinements by assumptions about the X-H bond lengths and the bond angles in which H atoms are involved.

$[H_3N(CH_2)_3NH_3]ZnBr_4$ (**1**)

Atom	x	y	z	U_{eq}
Zn	2526 (1)	8617 (1)	10006 (1)	388 (3)
$Br^{(1)}$	3799 (1)	9589 (1)	12126 (1)	484 (3)
$Br^{(2)}$	3953 (1)	7886 (1)	9059 (1)	558 (4)
$Br^{(3)}$	814 (1)	9980 (1)	8460 (1)	501 (4)
$Br^{(4)}$	1482 (1)	6860 (1)	10436 (1)	414 (3)
$N^{(1)}$	3284 (7)	7042 (7)	3819 (8)	459 (18)
$H^{(N1,1)}$	2831 (7)	6590 (7)	3089 (8)	551
$H^{(N1,2)}$	3750 (7)	6558 (7)	4518 (8)	551
$H^{(N1,3)}$	3853 (7)	7533 (7)	3689 (8)	551
$N^{(2)}$	2785 (8)	10140 (7)	6731 (8)	481 (19)
$H^{(N2,1)}$	2193 (8)	10584 (7)	6876 (8)	577
$H^{(N2,2)}$	3325 (8)	10631 (7)	6556 (8)	577
$H^{(N2,3)}$	3282 (8)	9697 (7)	7458 (8)	577
$C^{(1)}$	2328 (9)	7774 (9)	4085 (10)	502 (24)
$H^{(C1,1)}$	1698 (9)	7236 (9)	4205 (10)	602
$H^{(C1,2)}$	1812 (9)	8289 (9)	3314 (10)	602
$C^{(2)}$	3031 (10)	8560 (8)	5312 (9)	456 (22)
$H^{(C2,1)}$	3539 (10)	8045 (8)	6085 (9)	548
$H^{(C2,2)}$	3667 (10)	9094 (8)	5196 (9)	548
$C^{(3)}$	2047 (9)	9316 (9)	5568 (9)	508 (23)
$H^{(C3,1)}$	1496 (9)	9796 (9)	4777 (9)	610
$H^{(C3,2)}$	1449 (9)	8289 (9)	5752 (9)	610

$[n\text{-}CH_3(CH_2)_2NH_3]_2ZnBr_4$ (**2**)

Atom	x	y	z	U_{eq}
Zn	7723 (1)	2699 (1)	398 (1)	587 (3)
$Br^{(1)}$	10607 (1)	1661 (1)	763 (1)	677 (3)
$Br^{(2)}$	5758 (1)	1733 (1)	981 (1)	757 (3)
$Br^{(3)}$	6354 (1)	2303 (1)	−795 (1)	740 (3)
$Br^{(4)}$	8065 (2)	4893 (1)	638 (1)	962 (4)
$N^{(1)}$	3329 (12)	4459 (7)	1074 (4)	901 (25)
$H^{(N1,1)}$	2240 (19)	4564 (72)	780 (4)	1261
$H^{(N1,2)}$	3774 (98)	3716 (29)	1003 (13)	1261
$H^{(N1,3)}$	4064 (83)	5069 (47)	1018 (13)	1261
$N^{(2)}$	2329 (10)	3998 (8)	4424 (4)	846 (23)
$H^{(N2,1)}$	3416 (22)	3642 (38)	4509 (26)	1185
$H^{(N2,2)}$	1990 (51)	4011 (56)	4803 (12)	1185
$H^{(N2,3)}$	2380 (70)	4782 (20)	4278 (15)	1185
$C^{(1)}$	3181 (16)	4506 (13)	1757 (6)	1164 (41)
$H^{(C1,1)}$	2472 (16)	3785 (13)	1818 (6)	1397
$H^{(C1,2)}$	2495 (16)	5253 (13)	1794 (6)	1397
$C^{(2)}$	4864 (25)	4519 (17)	2327 (8)	1838 (75)
$H^{(C2,1)}$	4520 (25)	4435 (17)	2743 (8)	2206
$H^{(C2,2)}$	5542 (25)	3768 (17)	2287 (8)	2206
$C^{(3)}$	6058 (20)	5544 (16)	2413 (9)	1751 (73)
$H^{(C3,1)}$	6457 (140)	5637 (78)	2014 (29)	2451
$H^{(C3,2)}$	7084 (90)	5397 (59)	2800 (41)	2451
$H^{(C3,3)}$	5449 (58)	6298 (26)	2483 (68)	2451
$C^{(4)}$	1020 (16)	3274 (10)	3903 (6)	933 (32)
$H^{(C4,1)}$	1223 (16)	2386 (10)	4009 (6)	1120
$H^{(C4,2)}$	−184 (16)	3447 (10)	3928 (6)	1120
$C^{(5)}$	1063 (18)	3467 (15)	3231 (6)	1262 (46)
$H^{(C5,1)}$	2288 (18)	3320 (15)	3212 (6)	1514
$H^{(C5,2)}$	777 (18)	4343 (15)	3115 (6)	1514
$C^{(6)}$	−200 (20)	2659 (14)	2699 (7)	1439 (56)
$H^{(C6,1)}$	389 (58)	1880 (45)	2656 (40)	2015
$H^{(C6,2)}$	−520 (119)	3094 (45)	2271 (15)	2015
$H^{(C6,3)}$	−1273 (69)	2488 (87)	2830 (28)	2015

$[n\text{-}H_3C(CH_2)_3NH_3]_2ZnBr_4$ (**3**)

Atom	x	y	z	U_{eq}
Zn	2456 (2)	320 (1)	2687 (2)	804 (7)
$Br^{(1)}$	5010 (2)	656 (1)	1654 (2)	955 (7)
$Br^{(2)}$	2579 (3)	594 (1)	4835 (2)	1075 (8)
$Br^{(3)}$	−13 (2)	779 (1)	1640 (2)	1009 (7)
$Br^{(4)}$	2120 (3)	−747 (1)	2440 (2)	1077 (8)
$N^{(1)}$	2245 (22)	546 (7)	8976 (16)	1230 (57)
$N^{(2)}$	7519 (22)	870 (7)	4348 (13)	1047 (47)
$C^{(1)}$	3128 (33)	964 (13)	8196 (24)	1646 (116)
$C^{(2)}$	2410 (34)	1591 (13)	8428 (25)	1537 (92)
$C^{(3)}$	3179 (44)	2025 (14)	7507 (27)	2048 (140)
$C^{(4)}$	2578 (46)	2662 (13)	7660 (41)	2596 (225)
$C^{(5)}$	7088 (40)	1522 (10)	4405 (26)	1792 (120)
$C^{(6)}$	8534 (39)	1918 (14)	4776 (38)	2620 (228)
$C^{(7)}$	8041 (47)	2580 (12)	4600 (31)	2002 (140)
$C^{(8)}$	7066 (47)	2760 (14)	5689 (36)	2680 (235)

160 pm and 190 pm, respectively [12]. Two $[ZnBr_4]^{2-}$ tetrahedra receive the 9 hydrogen bonds formed with all of the hydrogen atoms in two different NH_3^+ groups. The $N^{(1)}H_3^+$ group is connected to $Br^{(1)}$(2 ×), $Br^{(3)}$, and $Br^{(4)}$(2 ×), and the $N^{(2)}H_3^+$ group to $Br^{(2)}$(2 ×), $Br^{(3)}$ and $Br^{(4)}$. The hydrogen bond network leads to the layer structure in the *ab* plane at $z = 0$ and $z = 1/2$, which layer is made up of the $[ZnBr_4]^{2-}$ anions and the cations through the hydrogen bonds. These layers are connected through $N^{(2)}–H \cdots Br^{(2)}$ hydrogen bonds.

$[n\text{-}H_3C(CH_2)_2NH_3]_2ZnBr_4$ (**2**)

Bis(*n*-propylammonium) tetrabromozincate(II) (**2**) crystallizes monoclinic with space group $C_{2h}^5\text{-}P2_1/c$ at 291 K; for the lattice constants etc., see Table 1. The atomic coordinates and displacement parameters are given in Table 2. Intramolecular distances and angles are listed in Tables 3 and 4. Figure 3 illustrates the formula unit with the thermal ellipsoids and their

Table 3. Intramolecular bond distances (in pm) and bond angles (in degree) for the tetrahedral coordinated $ZnBr_4^{2-}$ anions, and hydrogen bond scheme.

$[H_3N(CH_2)_3NH_3]ZnBr_4$ (**1**)

Connection	d/pm	Connection	Angle/°
$\mathrm{Zn{-}Br}^{(1)}$	238.9(2)	$\mathrm{Br}^{(1)}\mathrm{{-}Zn{-}Br}^{(2)}$	112.11(6)
$\mathrm{Zn{-}Br}^{(2)}$	240.6(2)	$\mathrm{Br}^{(1)}\mathrm{{-}Zn{-}Br}^{(3)}$	110.54(6)
$\mathrm{Zn{-}Br}^{(3)}$	241.7(2)	$\mathrm{Br}^{(1)}\mathrm{{-}Zn{-}Br}^{(4)}$	106.21(6)
$\mathrm{Zn{-}Br}^{(4)}$	240.7(1)	$\mathrm{Br}^{(2)}\mathrm{{-}Zn{-}Br}^{(3)}$	110.54(6)
		$\mathrm{Br}^{(2)}\mathrm{{-}Zn{-}Br}^{(4)}$	107.07(5)
		$\mathrm{Br}^{(3)}\mathrm{{-}Zn{-}Br}^{(4)}$	110.22(6)

Hydrogen bond scheme

Connection	d/pm	Angle ($\mathrm{N{-}H\cdots Br}$)/°
$\mathrm{N}^{(1)}\cdots\mathrm{Br}^{(1')}$	338.6	126.3
$\mathrm{H}^{(\mathrm{N}1,1)}\cdots\mathrm{Br}^{(1')}$	278.3	
$\mathrm{N}^{(1)}\cdots\mathrm{Br}^{(1'')}$	356.4	139.8
$\mathrm{H}^{(\mathrm{N}1,3)}\cdots\mathrm{Br}^{(1'')}$	283.7	
$\mathrm{N}^{(1)}\cdots\mathrm{Br}^{(3')}$	355.1	157.7
$\mathrm{H}^{(\mathrm{N}1,2)}\cdots\mathrm{Br}^{(3')}$	271.1	
$\mathrm{N}^{(1)}\cdots\mathrm{Br}^{(4')}$	338.6	139.2
$\mathrm{H}^{(\mathrm{N}1,1)}\cdots\mathrm{Br}^{(4')}$	266.3	
$\mathrm{N}^{(1)}\cdots\mathrm{Br}^{(4'')}$	338.4	129.1
$\mathrm{H}^{(\mathrm{N}1,3)}\cdots\mathrm{Br}^{(4'')}$	275.1	
$\mathrm{N}^{(2)}\cdots\mathrm{Br}^{(1''')}$	341.4	122.7
$\mathrm{H}^{(\mathrm{N}2,2)}\cdots\mathrm{Br}^{(1''')}$	284.9	
$\mathrm{N}^{(2)}\cdots\mathrm{Br}^{(2)}$	339.1	158.1
$\mathrm{H}^{(\mathrm{N}2,3)}\cdots\mathrm{Br}^{(2)}$	254.8	
$\mathrm{N}^{(2)}\cdots\mathrm{Br}^{(2')}$	346.6	132.2
$\mathrm{H}^{(\mathrm{N}2,1)}\cdots\mathrm{Br}^{(2')}$	280.6	
$\mathrm{N}^{(2)}\cdots\mathrm{Br}^{(3)}$	352.0	128.7
$\mathrm{H}^{(\mathrm{N}2,1)}\cdots\mathrm{Br}^{(3)}$	289.5	
$\mathrm{N}^{(2)}\cdots\mathrm{Br}^{(4''')}$	344.8	143.0
$\mathrm{H}^{(\mathrm{N}2,1)}\cdots\mathrm{Br}^{(4''')}$	269.5	

$\mathrm{Br}^{(1')}$: $-x+1/2,\ y-1/2,\ -z+3/2$; $\mathrm{Br}^{(1'')}$: $x,\ y,\ z-1$; $\mathrm{Br}^{(1''')}$: $-x+1,\ -y+2,\ -z+2$; $\mathrm{Br}^{(2')}$: $-x+1/2,\ y+1/2,\ -z+3/2$; $\mathrm{Br}^{(3')}$: $-x+1/2,\ y-1/2,\ -z+3/2$; $\mathrm{Br}^{(4')}$: $x,\ y,\ z-1$; $\mathrm{Br}^{(4'')}$: $x+1/2,\ -y+3/2,\ z-1/2$; $\mathrm{Br}^{(4''')}$: $-x+1/2,\ y+1/2,\ -z+3/2$.

$[n\text{-}H_3C(CH_2)_2NH_3]ZnBr_4$ (**2**)

Connection	d/pm	Connection	Angle/°
$\mathrm{Zn{-}Br}^{(1)}$	240.2(1)	$\mathrm{Br}^{(1)}\mathrm{{-}Zn{-}Br}^{(2)}$	107.9(1)
$\mathrm{Zn{-}Br}^{(2)}$	241.6(1)	$\mathrm{Br}^{(1)}\mathrm{{-}Zn{-}Br}^{(3)}$	109.4(1)
$\mathrm{Zn{-}Br}^{(3)}$	240.9(2)	$\mathrm{Br}^{(1)}\mathrm{{-}Zn{-}Br}^{(4)}$	110.3(1)
$\mathrm{Zn{-}Br}^{(4)}$	237.9(2)	$\mathrm{Br}^{(2)}\mathrm{{-}Zn{-}Br}^{(3)}$	106.0(1)
		$\mathrm{Br}^{(2)}\mathrm{{-}Zn{-}Br}^{(4)}$	111.1(1)
		$\mathrm{Br}^{(3)}\mathrm{{-}Zn{-}Br}^{(4)}$	111.8(1)

Table 3 (continued)

Hydrogen bond scheme

Connection	d/pm	Angle ($\mathrm{N{-}H\cdots Br}$)/°
$\mathrm{N}^{(1)}\cdots\mathrm{Br}^{(1')}$	357.8	108.4
$\mathrm{H}^{(\mathrm{N}1,2)}\cdots\mathrm{Br}^{(1')}$	320.7	
$\mathrm{N}^{(1)}\cdots\mathrm{Br}^{(2)}$	348.3	167.0
$\mathrm{H}^{(\mathrm{N}1,2)}\cdots\mathrm{Br}^{(2)}$	261.0	
$\mathrm{N}^{(1)}\cdots\mathrm{Br}^{(3')}$	350.7	133.7
$\mathrm{H}^{(\mathrm{N}1,3)}\cdots\mathrm{Br}^{(3')}$	283.2	
$\mathrm{N}^{(1)}\cdots\mathrm{Br}^{(4')}$	343.7	119.5
$\mathrm{H}^{(\mathrm{N}1,1)}\cdots\mathrm{Br}^{(4')}$	291.0	
$\mathrm{N}^{(2)}\cdots\mathrm{Br}^{(1'')}$	345.4	161.5
$\mathrm{H}^{(\mathrm{N}2,1)}\cdots\mathrm{Br}^{(1'')}$	259.8	
$\mathrm{N}^{(2)}\cdots\mathrm{Br}^{(1''')}$	357.4	121.2
$\mathrm{H}^{(\mathrm{N}2,3)}\cdots\mathrm{Br}^{(1''')}$	303.1	
$\mathrm{N}^{(2)}\cdots\mathrm{Br}^{(2')}$	346.7	151.0
$\mathrm{H}^{(\mathrm{N}2,3)}\cdots\mathrm{Br}^{(2')}$	266.1	
$\mathrm{N}^{(2)}\cdots\mathrm{Br}^{(2'')}$	360.0	120.1
$\mathrm{H}^{(\mathrm{N}2,1)}\cdots\mathrm{Br}^{(2'')}$	307.0	
$\mathrm{N}^{(2)}\cdots\mathrm{Br}^{(3'')}$	354.4	156.2
$\mathrm{H}^{(\mathrm{N}2,2)}\cdots\mathrm{Br}^{(3'')}$	271.2	

$\mathrm{Br}^{(1')}$: $x-1,\ y,\ z$; $\mathrm{Br}^{(1'')}$: $x-1,\ -y+1/2,\ z+1/2$; $\mathrm{Br}^{(1''')}$: $-x+1,\ y+1/2,\ -z+1/2$; $\mathrm{Br}^{(2')}$: $-x+1,\ y+1/2,\ -z+1/2$; $\mathrm{Br}^{(2'')}$: $x,\ -y+1/2,\ z+1/2$; $\mathrm{Br}^{(3')}$: $-x+1,\ -y+1,\ -z$; $\mathrm{Br}^{(3'')}$: $x,\ -y+1/2,\ z+1/2$; $\mathrm{Br}^{(4')}$: $-x+1,\ -y+1,\ -z$.

$[n\text{-}H_3C(CH_2)_3NH_3]ZnBr_4$ (**3**)

Connection	d/pm	Connection	Angle/°
$\mathrm{Zn{-}Br}^{(1)}$	240.3(3)	$\mathrm{Br}^{(1)}\mathrm{{-}Zn{-}Br}^{(2)}$	110.8(1)
$\mathrm{Zn{-}Br}^{(2)}$	238.1(3)	$\mathrm{Br}^{(1)}\mathrm{{-}Zn{-}Br}^{(3)}$	107.3(1)
$\mathrm{Zn{-}Br}^{(3)}$	240.5(3)	$\mathrm{Br}^{(1)}\mathrm{{-}Zn{-}Br}^{(4)}$	110.2(1)
$\mathrm{Zn{-}Br}^{(4)}$	240.6(3)	$\mathrm{Br}^{(2)}\mathrm{{-}Zn{-}Br}^{(3)}$	110.5(1)
		$\mathrm{Br}^{(2)}\mathrm{{-}Zn{-}Br}^{(4)}$	111.2(1)
		$\mathrm{Br}^{(3)}\mathrm{{-}Zn{-}Br}^{(4)}$	106.8(1)

Hydrogen bond scheme

Connection	d/pm
$\mathrm{N}^{(1)}\cdots\mathrm{Br}^{(1')}$	349.1
$\mathrm{N}^{(1)}\cdots\mathrm{Br}^{(1'')}$	352.8
$\mathrm{N}^{(1)}\cdots\mathrm{Br}^{(3')}$	342.5
$\mathrm{N}^{(1)}\cdots\mathrm{Br}^{(3'')}$	347.1
$\mathrm{N}^{(1)}\cdots\mathrm{Br}^{(4')}$	367.0
$\mathrm{N}^{(2)}\cdots\mathrm{Br}^{(1)}$	345.8
$\mathrm{N}^{(2)}\cdots\mathrm{Br}^{(2')}$	338.2
$\mathrm{N}^{(2)}\cdots\mathrm{Br}^{(3''')}$	352.0
$\mathrm{N}^{(2)}\cdots\mathrm{Br}^{(4'')}$	345.6

$\mathrm{Br}^{(1')}$: $-x+1,\ -y,\ -z+1$; $\mathrm{Br}^{(1'')}$: $x,\ y,\ z+1$; $\mathrm{Br}^{(2')}$: $-x+1,\ -y,\ -z+1$; $\mathrm{Br}^{(3')}$: $x,\ y,\ z+1$; $\mathrm{Br}^{(3'')}$: $-x,\ -y,\ -z+1$; $\mathrm{Br}^{(3''')}$: $x+1,\ y,\ z$; $\mathrm{Br}^{(4')}$: $-x,\ -y,\ -z+1$; $\mathrm{Br}^{(4'')}$: $-x+1,\ -y,\ -z+1$.

atomic numbering used in this paper. The projection of the unit cell of (**2**) along [100] onto the *bc* plane is shown in Figure 4. The $[ZnBr_4]^{2-}$ tetrahedron is slightly distorted. The Zn–Br distances and Br–Zn–Br angles are found $237.9 \le d(\mathrm{Zn{-}Br})/\mathrm{pm} \le 241.6$ (mean value 240.1 pm) and $106.0 \le \angle(\mathrm{Br{-}Zn{-}Br})/° \le 111.8$ (mean value 109.5°), respectively, as listed in Table 3. Two *n*-propylammonium cations in the formula unit are crystallographically inequivalent. The displacement parameters of the carbon atoms are very large as listed in Table 2. This is related to the disorder of the cations as in the room temperature phase of bis(*n*-

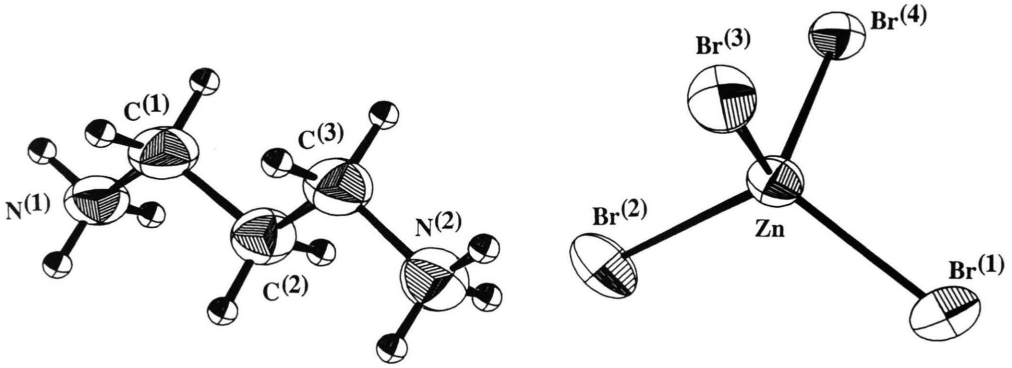

Fig. 1. Formula unit of 1,3-propanediammonium tetrabromozincate(II) (**1**) with the numbering of the atoms. The thermal ellipsoids (50% of electrons as contour) are shown, too.

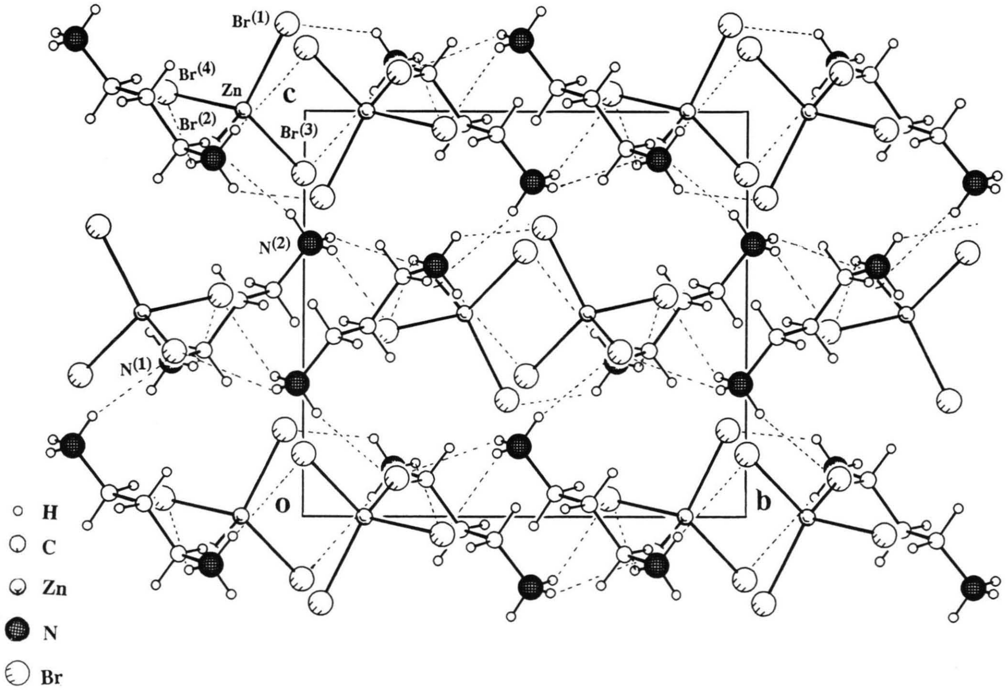

Fig. 2. Projection of the unit cell of (**1**) along [100] onto the *bc* plane. Hydrogen bonds are marked by dashed lines.

propylammonium) tetrachlorozincate(II) [13]. Considerable disorder has been observed in the *n*-propylammonium ions which leads to an unacceptable spread in the C–C bond distances. The final refinement has therefore been carried out with C–C distances restrained to their theoretical values. There is an interesting difference between the structures of the two independent cations in (**2**). The cation 2($N^{(2)}$) shows the normal *trans* chain structure, whereas the cation 1($N^{(1)}$) has a kink in the chain, i.e., a *gauche* conformation for the terminal methyl groups. Interestingly the carbon atoms in cation 1 have larger displacement parameters than those in cation 2. We have calculated the torsion angles for the two cations given in Table 4. A *gauche* conformation of the alkyl chain has not been observed in the structure of the chloride analogue [13].

In Table 3 distances and angles of the N–H···Br hydrogen bonds in (**2**) are listed in consideration of the sum of the van der Waals radii of the NH_4^+ group and

Table 4. Intramolecular distances (in pm) and angles (in degree) within the alkylenediammonium or alkylammonium cations.

$[H_3N(CH_2)_3NH_3]ZnBr_4$ (**1**)

Connection	*d*/pm	Connection	Angle/°
$N^{(1)}-C^{(1)}$	146.3(12)	$N-C^{(1)}-C^{(2)}$	112.2 (8)
$C^{(1)}-C^{(2)}$	150.4(13)	$C^{(1)}-C^{(2)}-C^{(3)}$	111.9 (8)
$C^{(2)}-C^{(3)}$	149.8(13)	$C^{(2)}-C^{(3)}-N^{(2)}$	110.2 (8)
$C^{(3)}-N^{(2)}$	148.6(11)		

The distances $N^{(1)}-H^{(N1)}$ and $N^{(2)}-H^{(N2)}$ are fixed to 89 pm. The distances $C^{(1)}-H^{(C1)}$, $C^{(2)}-H^{(C2)}$, and $C^{(3)}-H^{(C3)}$ are fixed to 97 pm. The angles $H-N^{(1)}-H$ and $H-N^{(2)}-H$ are fixed to 109.5(5)°. The following angles are also fixed; $C^{(1)}-N^{(1)}-H$, 109.3–109.5°; $C^{(3)}-N^{(2)}-H$, 109.4–109.6°; $H-C^{(1)}-H$, 107.9°; $H-C^{(2)}-H$, 108.1°; $H-C^{(3)}-H$, 108.1°.

$[n\text{-}H_3C(CH_2)_2NH_3]_2ZnBr_4$ (**2**)

Connection	*d*/pm	Connection	Angle/°
$N^{(1)}-C^{(1)}$	140.0(13)	$N^{(1)}-C^{(1)}-C^{(2)}$	118.3(12)
$C^{(1)}-C^{(2)}$	147.7(14)	$C^{(1)}-C^{(2)}-C^{(3)}$	120.1(15)
$C^{(2)}-C^{(3)}$	140.4(15)		
$N^{(2)}-C^{(4)}$	146.2(12)	$N^{(2)}-C^{(4)}-C^{(5)}$	115.8(10)
$C^{(4)}-C^{(5)}$	140.5(15)	$C^{(4)}-C^{(5)}-C^{(6)}$	115.9(12)
$C^{(5)}-C^{(6)}$	150.5(17)		

Selected torsion angles:

Connecting planes	Angle/°
$N^{(1)}C^{(1)}C^{(2)} \mid C^{(1)}C^{(2)}C^{(3)}$	64.9(24)
$N^{(2)}C^{(4)}C^{(5)} \mid C^{(4)}C^{(5)}C^{(6)}$	176.1(11)

$[n\text{-}H_3C(CH_2)_3NH_3]_2ZnBr_4$ (**3**)

Connection	*d*/pm	Connection	Angle/°
$N^{(1)}-C^{(1)}$	143.5(16)	$N^{(1)}-C^{(1)}-C^{(2)}$	108.6(20)
$C^{(1)}-C^{(2)}$	152.7(18)	$C^{(1)}-C^{(2)}-C^{(3)}$	109.2(20)
$C^{(2)}-C^{(3)}$	151.5(18)	$C^{(2)}-C^{(3)}-C^{(4)}$	113.8(27)
$C^{(3)}-C^{(4)}$	150.3(18)		
$N^{(2)}-C^{(5)}$	149.1(17)	$N^{(2)}-C^{(5)}-C^{(6)}$	115.5(24)
$C^{(5)}-C^{(6)}$	146.6(18)	$C^{(5)}-C^{(6)}-C^{(7)}$	111.3(25)
$C^{(6)}-C^{(7)}$	153.4(19)	$C^{(6)}-C^{(7)}-C^{(8)}$	107.2(28)
$C^{(7)}-C^{(8)}$	146.2(19)		

Selected torsion angles:

Connecting planes	Angle/°
$N^{(1)}C^{(1)}C^{(2)} \mid C^{(1)}C^{(2)}C^{(3)}$	−173.6(23)
$C^{(1)}C^{(2)}C^{(3)} \mid C^{(2)}C^{(3)}C^{(4)}$	−179.2(29)
$N^{(2)}C^{(5)}C^{(6)} \mid C^{(5)}C^{(6)}C^{(7)}$	170.6(25)
$C^{(5)}C^{(6)}C^{(7)} \mid C^{(6)}C^{(7)}C^{(8)}$	81.7(40)

the Br atom, 350 pm [12]. All amino hydrogen atoms are connected to bromine atoms. The $N^{(1)}H_3^+$ group was connected to $Br^{(1)}$, $Br^{(2)}$, $Br^{(3)}$, and $Br^{(4)}$ and the $N^{(2)}H_3^+$ group to $Br^{(1)}(2\times)$, $Br^{(2)}(2\times)$, and $Br^{(3)}$. The hydrogen bond network leads to the layer structure made up of the $[ZnBr_4]^{2-}$ anions and the cations lying in the *ab* plane centered at $z=0$ and $z=1/2$. The hydrogen bonds were formed within these planes, while the layers are connected by van der Waals interactions.

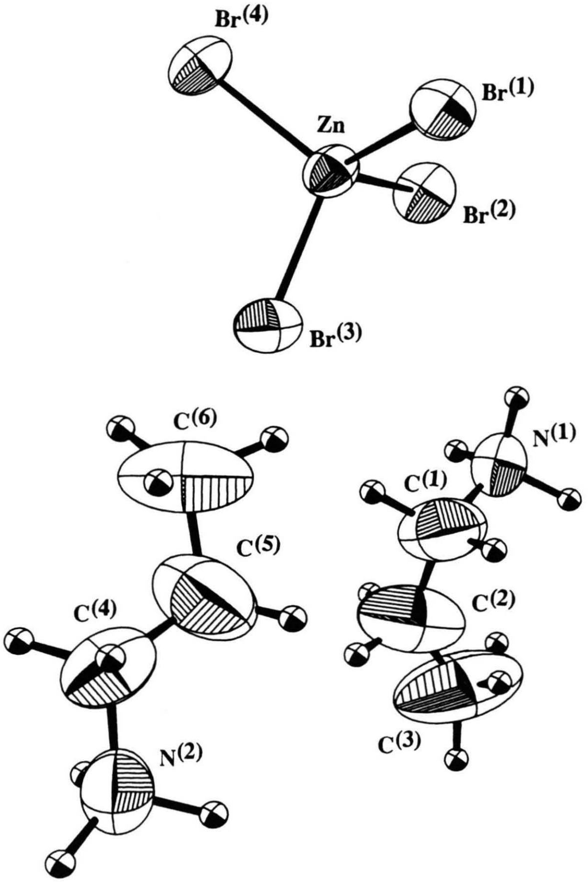

Fig. 3. Formula unit of *n*-propylammonium tetrabromozincate(II) (**2**) with the numbering of the atoms. The thermal ellipsoids (50% of electrons as contour) are shown, too.

$[n\text{-}H_3C(CH_2)_3NH_3]_2ZnBr_4$ (3)

Bis(*n*-butylammonium) tetrabromozincate(II) (**3**) crystallizes monoclinic with space group C_{2h}^5-$P2_1/c$ at 295 K. In Fig. 5 we show a sketch of one formula unit with thermal ellipsoids. The lattice constants etc. are shown in Table 1, and the atomic coordinates and thermal parameters in Table 2. In Fig. 6 the unit cell is projected along [100] on the *bc* plane. Intramolecular distances are found in Tables 3 and 4. The characteristic feature of (**3**) is the isolated tetrahedral structure of

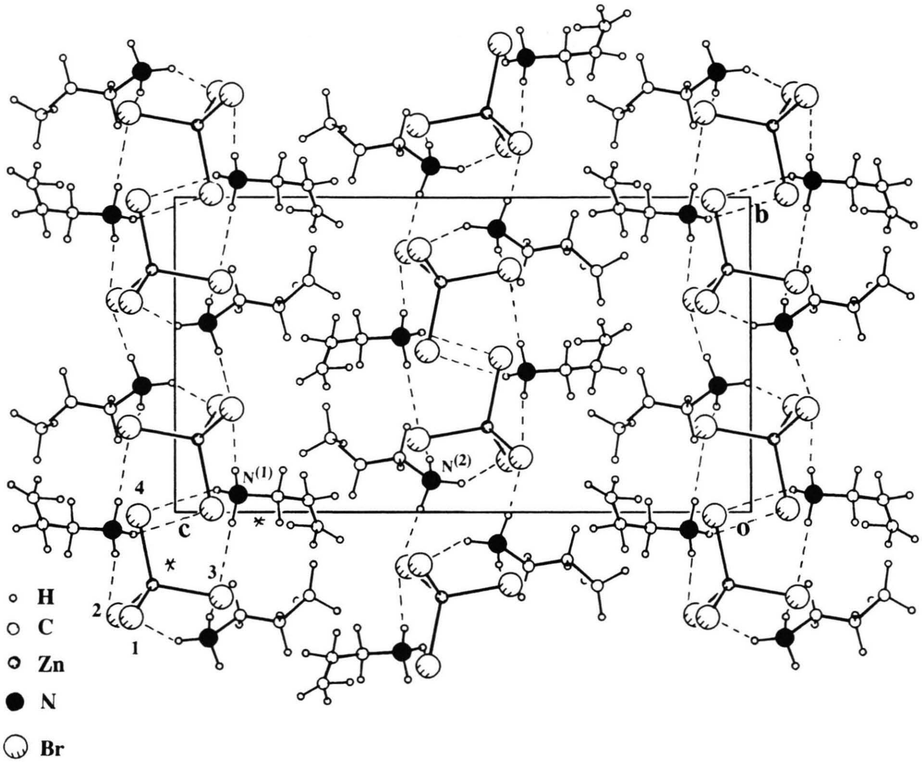

Fig. 4. Projection of the unit cell of (**2**) along [100] onto the *bc* plane. Hydrogen bonds are marked by dashed lines.

$[ZnBr_4]^{2-}$ as observed for (**1**) and (**2**). Again, the $[ZnBr_4]^{2-}$ tetrahedron deviates little from regularity: $238.1 \leq d(\text{Zn–Br})/\text{pm} \leq 240.6$ (mean value 239.9 pm), and $106.8 \leq \angle(\text{Br–Zn–Br})/°111.2$ (mean value 109.5°). There are two crystallographically inequivalent *n*-butylammonium cations in the unit cell as in the structure of (**2**). The displacement parameters of carbon atoms are very large like in (**2**). The compound (**3**) undergoes the order-disorder phase transition with a second-order character at 299 K [9]. The disorder in the cation lead to a considerable shortening of the C–C distance as previously reported by [14]. Therefore in analogy to (**2**) the refinement in the final cycles was restrained to theoretical values of C–C bonds. Like in (**2**), there is an interesting difference between the structures of the two independent cations in (**3**). The cation $1(\text{N})^{(1)}$) shows a whole *trans* chain structure, while the cation $2(\text{N})^{(2)}$) has a kink in the chain, i.e., a *gauche* conformation for the terminal methyl group (see Table 4). In addition, the

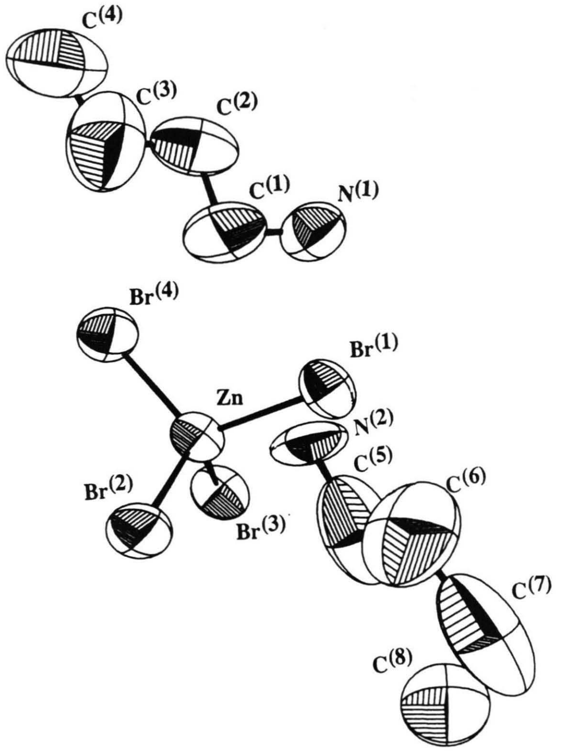

Fig. 5. Formula unit of *n*-butylammonium tetrabromozincate(II) (**3**) with the numbering of the atoms. The thermal ellipsoids (50% of electrons as contour) are shown, too.

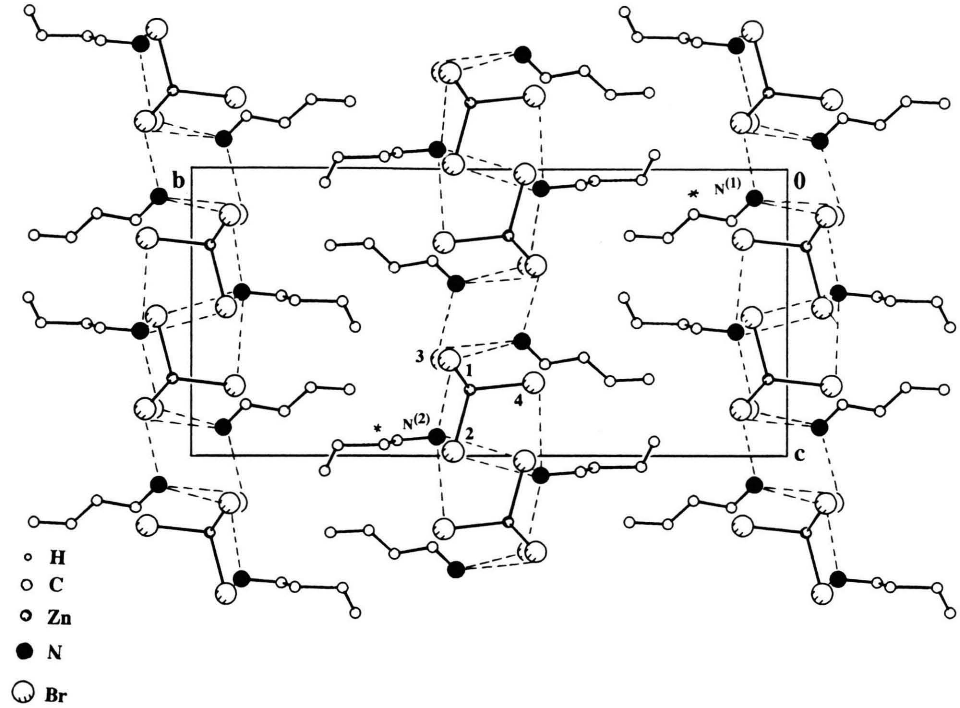

Fig. 6. Projection of the unit cell of (3) along [100] onto the *bc* plane. Hydrogen bonds are marked by dashed lines.

carbon atoms in the cation 2 have larger displacement parameters than those ion the cation 1.

We have calculated some hydrogen bond distances N···Br, see Table 3. The $N^{(1)}H_3^+$ group was connected to $Br^{(1)}(2\times)$, $Br^{(3)}(2\times)$, and $Br^{(4)}$, and the $N^{(2)}H_3^+$ group to $Br^{(1)}$, $Br^{(2)}$, $Br^{(3)}$ and $Br^{(4)}$. The hydrogen bond network leads to the following layered structure of (**3**): the $[ZnBr_4]^{2-}$ tetrahedra are located in the *ac* plane, centered at $y=0$ and $y=0.5$, and they are connected by the hydrogen bonds to the cations making a two-dimensional system. The layers are held together at $y=0.25$ and $y=0.75$ by van der Waals interactions. Therefore, the main structure is very similar to the structure of (**2**).

^{81}*Br Nuclear Quadrupole Resonance and Phase Transitions*

DSC measurements on (**1**) in the temperature range between 130 K and the melting point of 577 K show that the compound (**1**) undergoes a phase transition at 474 K. The ^{81}Br NQR spectrum in the phase II of (**1**) consists of a quartet, i.e., four lines with the same intensity, which is in agreement with the result of our crystal structure determination of (**1**) at room temperature. The numerical data are given in Table 5 and the temperature dependence of NQR frequencies measured between 77 and 350 K is shown in Figure 7. The ^{81}Br NQR and DSC measurement of (**2**) and (**3**) have been carried out recently as a function of temperature [9, 15]. At room temperature both compounds show a quartet of ^{81}Br NQR spectrum, which is in agreement with the results of our crystal structure determinations. The compound (**2**) shows a rather complicated phase diagram. The phase transition takes place at 347 K [15]. Although it was concluded that a phase transition is located at 298 K by NQR measurements [9], no heat anomaly was observed around 298 K on DSC measurements [15]. There is another phase transition at 130 K, and at least one more transition occurs in the temperature range between 77 and 120 K [9]. On the other hand, only one transition was found for (**3**) at $T_{II,I}=299$ K. For more elaborated discussions of the phase transitions and ^{81}Br NQR of (**2**) and (**3**), and along with literature on $(C_nH_{2n+1}NH_3)_2ZnBr_4$ compounds, see [9] and [15].

^{81}Br NQR results of $[H_3N(CH_2)_4NH_3]ZnBr_4$ (**4**) and $[n\text{-}H_3C(CH_2)_4NH_3]_2NH_3]_2ZnBr_4$ (**5**) show that

Table 5. ^{81}Br NQR frequencies at selected temperatures and coefficients a_i of the power series with the least squares approximation $\nu(^{81}\mathrm{Br})=\sum_i a_i \times T^i$, $-1 \leq i \leq 2$ of $[\mathrm{H_3N(CH_2)_3NH_3}]$ $\mathrm{ZnBr_4}$ (**1**). Z is the number of experimental points, σ is the mean squares deviation. The ^{81}Br NQR results are also listed for $[\mathrm{H_3N(CH_2)_4NH_3}]$ $\mathrm{ZnBr_4}$ (**4**) and $[n\text{-}\mathrm{H_3C(CH_2)_4NH_3}]_2$ $\mathrm{ZnBr_4}$ (**5**) in phase II.

Frequencies at selected temperatures.

$[\mathrm{H_3N(CH_2)_3NH_3}]$ $\mathrm{ZnBr_4}$ (**1**)

ν_i	ν/MHz (T/K)	ν/MHz (T/K)
ν_1	61.634(77)	58.799(330)
ν_2	58.062(77)	57.328(330)
ν_3	56.675(77)	55.978(330)
ν_4	53.673(77)	52.365(330)

$[\mathrm{H_3N(CH_2)_4NH_3}]$ $\mathrm{ZnBr_4}$ (**4**)

ν_i	ν/MHz (T/K)	ν/MHz (T/K)
ν_1	65.992(77)	63.787(320)
ν_2	65.544(77)	62.963(320)
ν_3	59.900(77)	59.928(320)
ν_4	50.189(77)	50.364(320)

$[n\text{-}\mathrm{H_3C(CH_2)_4NH_3}]$ $\mathrm{ZnBr_4}$ (**5**)

ν_i	ν/MHz (T/K)	ν/MHz (T/K)
ν_1	61.279(77)	59.712(240)
ν_2	58.933(77)	56.936(240)
ν_3	57.869(77)	57.409(240)
ν_4	56.485(77)	54.793(240)

Coefficients of a_i of power series

$[\mathrm{H_3N(CH_2)_3NH_3}]\mathrm{ZnBr_4}$ (**1**) ($77 \leq T/\mathrm{K} \leq 341$)

ν_i	Z	σ	a_0	a_{-1}	$a_1 \cdot 10^3$	$a_2 \cdot 10^6$
		kHz	MHz	MHz K	MHz K^{-1}	MHz K^{-2}
ν_1	68	32	62.604	−3.063	−11.644	0.750
ν_2	68	29	58.314	−5.749	−3.451	1.755
ν_3	52	31	56.842	−2.087	−2.927	0.889
ν_4	41	29	53.871	−0.452	−2.658	−5.921

$[\mathrm{H_3N(CH_2)_4NH_3}]\mathrm{ZnBr_4}$ (**4**) ($77 \leq T/\mathrm{K} \leq 330$)

ν_i	Z	σ	a_0	a_{-1}	$a_1 \cdot 10^3$	$a_2 \cdot 10^6$
		kHz	MHz	MHz K	MHz K^{-1}	MHz K^{-2}
ν_1	53	40	66.475	0.007	−5.708	−8.179
ν_2	44	45	67.019	−43.873	−11.045	−3.860
ν_3	47	51	59.974	0.711	−2.972	8.920
ν_4	46	46	51.390	−50.000	−9.174	19.548

$[n\text{-}\mathrm{H_3C(CH_2)_4NH_3}]_2\mathrm{ZnBr_4}$ (**5**) ($77 \leq T/\mathrm{K} \leq 244$)

ν_i	Z	σ	a_0	a_{-1}	$a_1 \cdot 10^3$	$a_2 \cdot 10^6$
		kHz	MHz	MHz K	MHz K^{-1}	MHz K^{-2}
ν_1	25	40	61.963	0.339	−8.053	−5.526
ν_2	35	39	59.844	−0.675	−11.673	−2.560
ν_3	42	26	56.052	80.716	13.410	−37.791
ν_4	19	48	55.870	4.889	11.889	−66.557

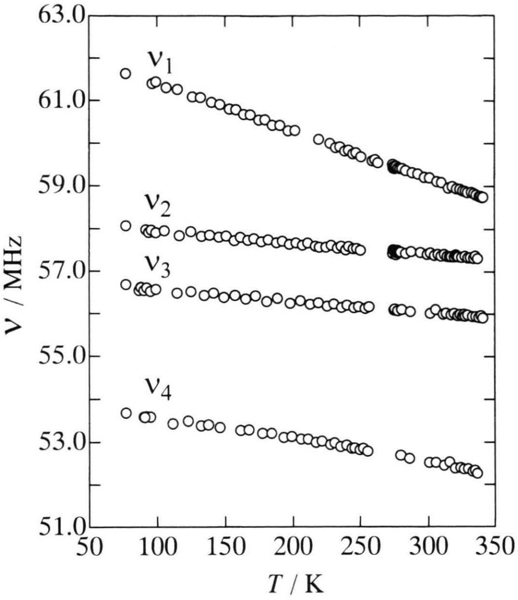

Fig. 7. Temperature dependence of ^{81}Br NQR frequencies of 1,3-propanediammonium tetrabromozincate(II) (**1**).

the spectrum of each compound consists of four lines with the same intensity as in (**1**)–(**3**) [9]. This fact seems to suggest that (**4**) and (**5**) have an isolated $[\mathrm{ZnBr_4}]^{2-}$ structure, too. The temperature dependences of NQR frequencies in (**4**) and (**5**) are shown in Figs. 8 and 9, respectively. A quartet in the ^{81}Br NQR spectrum of (**4**) could be observed between 77 and 330 K, above which temperature four NQR lines disappeared. DSC measurement shows several phase transitions located at 349 K and higher temperatures. The disappearance of NQR lines is due to the phase transition at 349 K and/or the activation of reorientational motions of $[\mathrm{ZnBr_4}]^{2-}$ anions. A quartet in the ^{81}Br NQR spectrum of (**5**) could be observed between 77 and 244 K, above which temperature three resonance lines disappeared. The NQR frequency of the remaining one line changed discontinuously at 244 K and it could be observed up to 255 K. This fact suggests that the phase transition is of first-order, which agrees with the results of DSC experiments [15]. The transitions observed at 347 K in (**2**), 299 K in (**3**), and 244 K in (**5**) are well explained by an order-disorder phase transition with a double-minimum potential for the alkylammonium orientation. However, the former two transitions are of the second-order type whereas the last is of the first-order type [15].

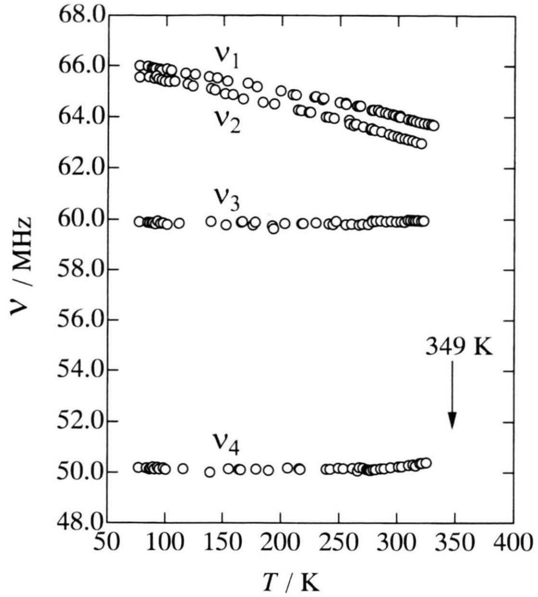

Fig. 8. Temperature dependence of ^{81}Br NQR frequencies of 1,4-butanediammonium tetrabromozincate(II) (**4**).

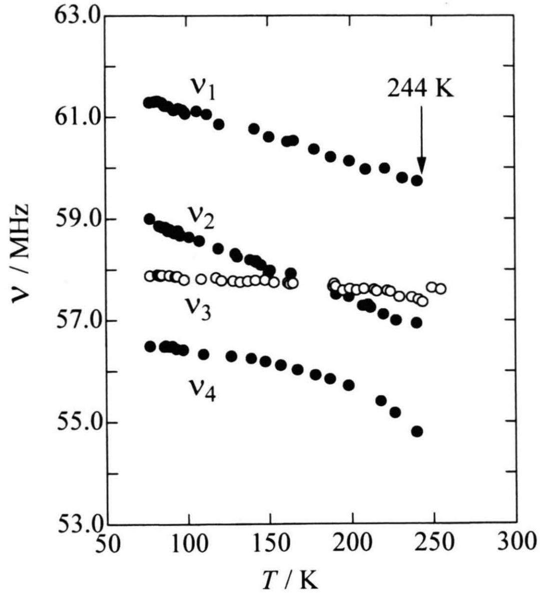

Fig. 9. Temperature dependence of ^{81}Br NQR frequencies of *n*-pentylammonium tetrabromozincate(II) (**5**).

Discussion

In the three $[ZnBr_4]^{2-}$ complexes reported in this paper, the $[ZnBr_4]^{2-}$ anion geometry is nearly identical. As seen from Table 3, the Zn–Br distances vary little among the three compounds, with the minimum of 237.9 pm in (**2**) and the maximum of 241.7 in (**1**). The average Zn–Br distance is between 239.9 pm for (**3**) and 240.5 pm for (**1**). Similarly, the tetrahedral angles Br–Zn–Br are only slightly different among the three compounds between 106.0° in (**2**) and 112.1° in (**1**). A mean angle of 109.45° is found for the three compounds. The small differences are probably due to the variations in the N–H···Br hydrogen bonds. For further discussion we need precise hydrogen positions as may be obtained by neutron diffraction.

We have information about the structure and the phase transitions of Rb_2ZnCl_4 which crystallizes with isolated tetrahedra $[ZnCl_4]^{2-}$ [16, 17] and shows interesting phase transitions. $[N(Ch_3)_4]_2ZnCl_4$ and $[N(CH_3)_4]_2ZnBr_4$ belong also to the class of A_2MX_4 complex salts with isolated tetrahedral anions, i.e., the β-K_2SO_4 structure [18, 19]. The compounds $[RNH_3]_2ZnCl_4$ with R = methyl [20], ethyl [21], *n*-propyl [13], *n*-dodecyl [22], and *n*-tetradecyl [23] exhibit isolated tetrahedra $[ZnCl_4]^{2-}$, arranged in the planes which are connected with the planes of the alkylammonium ions through N–H···Cl hydrogen bonds. Moreover, we found that $[RNH_3]_2ZnBr_4$ with R = *n*-propyl, *n*-butyl, and *n*-pentyl, and $[H_3NR'NH_3]ZnBr_4$ with R' = trimethylene and tetramethylene, and $[(CH_3)_2NH_2]_2ZnBr_4$ [6] have isolated tetrahedral anion structures. We can therefore conclude that $(A)_2Znx_4$ and $(A')ZnX_4$ complexes have an isolated tetrahedral anion structure without exception, and that the influence of the cations does not appear in $[ZnX_4]^{2-}$ compounds.

Tetrachloro complex salts of the metal ions of Mn(II), Cu(II), Cd(II), and Fe(II) formed with cations of $[RNH_3]^+$ and $[H_3NR'NH_3]^{2+}$ have been described in considerable number in the literature during the last 20 years. It is characteristic for these compounds that they have structures made up of layers of condensed octahedra $[MCl_6]_\infty$ [24]. The alkylammonium and alkylenediammonium cations are situated between the planar perovskite-type layers $[MCl_6]_\infty$, and the NH_3^+ groups form hydrogen bonds with the halogen atoms in the anion layers [24, 25]. The structures and magnetic properties of copper(II) halide (Cl, Br) complexes are comprehensively discussed in [25]. Besides the interesting magnetic properties [26–28], the compounds with M = Mn(II), Fe(II) and Cu(II) show phase transitions driven by the dynamics of the NH_3^+ groups which form the hydrogen bonds, and of the aliphatic part of cations. On the other hand, $[CdX_4]^{2-}$

complexes with $[RNH_3]^+$ or $[H_3NR'NH_3]^{2+}$ can take one of two types of structures, i.e., the perovskite-type layer structure and the isolated tetrahedral anion structure, depending on the number of hydrogen bonds between the anion and the cation, and also on the cation size [6, 8]. Furthermore, $[1,4\text{-}(H_3N)_2C_6H_4]CdBr_4$ can take another type of anion coordination, i.e., $[CdBr_5]_\infty$ [8].

Based on the results presented above, we may conclude that $[ZnX_4]^{2-}$ complexes form only isolated tetrahedral anions. This is probably a consequence of the pronounced preference of the $[ZnX_4]^{2-}$ tetrahedral coordination in zinc halide compounds. For example, $[M(NH_3)_6]ZnCl_5$ (M(III) = Co, Cr) has a structure which consists of tetrahedral $[ZnCl_4]^{2-}$ ions with an additional Cl^- anion [29, 30]. In contrast, $[M(NH_3)_6]CdCl_5$ (M(III) = Co, Cr) has the trigonal bipyramidal $[CdCl_5]^{3-}$ structure [31, 32]. What are therefore the driving forces for the polymerisation of the complex $[MX_4]^{2-}$ which lead to two-dimensional perovskite type layers? We may state that the basic building unit of the layers is octahedral with distorsions towards tetragonal coordination. This structure is observed in the complex salts of Mn, Cu, Fe and Cd. It seems, therefore, that this structure type is energetically more favorable than isolated tetrahedra. In addition, the bridging power of halogen atoms in the complexes is strong enough to form two-dimensional networks. In order to elucidate the difference between the behavior of Zn and Cd complex salts further subsequent molecular orbital calculations are to be carried out.

Acknowledgements

Two of us, H. I. and K. H., are thankful to the Alexander von Humboldt-Stiftung for a fellowship. The support of the Fonds der Chemischen Industrie and of the Deutsche Forschungsgemeinschaft is acknowledged, too.

[1] V. G. Krishnan and Al. Weiss, J. Mol. Struct. **176,** 323 (1988).

[2] V. G. Krishnan, Shi-qi Dou, H. Paulus, and Al. Weiss, Ber. Bunsenges. Phys. Chem. **95,** 1256 (1991).

[3] V. G. Krishnan, Shi-qi Dou, and Al. Weiss, Z. Naturforsch. **46 a,** 1063 (1991).

[4] H. Ishihara, V. G. Krishnan, Shi-qi Dou, and Al. Weiss, Z. Naturforsch. **49 a,** 213 (1994).

[5] V. G. Krishnan, Shi-qi Dou, and Al. Weiss, Z. Naturforsch. **49 a,** 223 (1994).

[6] H. Ishihara, Shi-qi Dou, K. Horiuchi, V. G. Krishnan, H. Paulus, H. Fuess, and Al. Weiss, Z. Naturforsch. **51 a,** 1027 (1996).

[7] H. Ishihara, K. Horiuchi, K. Yamada, T. Okuda, V. G. Krishnan, and Al. Weiss, Chem. Lett. **1996,** 371.

[8] H. Ishihara, Shi-qi Dou, K. Horiuchi, V. G. Krishnan, H. Paulus, H. Fuess, and Al. Weiss, Z. Naturforsch. **51 a,** in press.

[9] K. Horiuchi and Al. Weiss, J. Mol. Struct. **345,** 97 (1995).

[10] G. M. Sheldrick, SHELX86. Program for the solution of crystal structures, Univ. of Göttingen, Germany 1986. SHELX93. Program for crystal structure determination, Univ. of Göttingen, Germany 1993.

[11] Further information on the crystal structure determinations may be obtained from the Fachinformationszentrum Karlsruhe, Gesellschaft für wissenschaftlich-technische Information mbH, D-76344 Eggenstein-Leopoldshafen, Germany. Inquiries should be accompanied by the depository number CSD-59419, the names of the authors and the full literature reference.

[12] A. Bondi, J. Phys. Chem. **68,** 441 (1964). L. Pauling, The Nature of the Chemical Bond, 3rd ed. Cornell University Press, Ithaca, New York 1960. – Al. Weiss and H. Witte, Kristallstruktur und chemische Bindung, Verlag Chemie, Weinheim 1983.

[13] F. J. Zuniga, M. J. Tello, J. M. Perez Mato, and M. A. Perez Jubindo, J. Chem. Phys. **76,** 2610 (1982).

[14] G. Chapuis, Acta Crystallogr. **B34,** 1506 (1978).

[15] Y. Sakiyama, K. Horiuchi, and R. Ikeda, J. Phys.: Condens. Matter. **8,** 5345 (1996).

[16] S. Sawada, Y. Shiroishi, A. Yamamoto, M. Takashige, and M. Matsuo, J. Phys. Soc. Japan **43,** 2099 (1977).

[17] S. Sawada, Y. Shiroishi, and A. Yamamoto, Ferroelectrics **21,** 413 (1978).

[18] M. Kahrizi and M. O. Steinnitz, Solid State Commun. **74,** 333 (1990).

[19] P. Trouelan, J. Lefebvre, and P. Derollez, Acta Crystallogr. **C40,** 386, (1984).

[20] J. M. Perez Mato, J. L. Manes, J. Fernandez, F. J. Zuniga, M. J. Tello, C. Sicoias, and M. A. Arriandiga, Phys. Status Solidi a, **68,** 29 (1981).

[21] B. Morosin and K. Emerson, Acta Crystallogr. **B32,** 294 (1976).

[22] M. R. Ciajolo, P. Corradini, and A. Pavone, Acta Crystallogr. **B33,** 553 (1977).

[23] F. J. Zuniga and G. Chapuis, Cryst. Struct. Commun. **10,** 533 (1981).

[24] J. J. Foster and N. S. Gill, J. Chem. Soc. A 2625 (1968); J. C. Crowley, H. W. Dodgen, and R. D. Willett, J. Phys. Chem., **86,** 4046 (1982); G. Chapuis, Phys. Status Solidi a, **43,** 203 (1977).

[25] R. Willet, H. Place, and M. Middleton, J. Amer. Chem. Soc. **110,** 8639 (1988).

[26] J. Koppen, R. Hamersams, J. V. Lebesque, and A. R. Miedema, Phys. Lett. **A 25,** 376 (1967).

[27] W. D. vam Amstel and L. J. de Jongh, Solid State Commun. **11,** 1423 (1972).

[28] L. J. de Jongh and A. R. Miedema, Adv. Phys. **23,** 1 (1974).

[29] D. W. Meek and J. A. Ibers, Inorg. Chem., **9,** 465 (1970).

[30] W. Clegg, Acta Crystallogr. **B32,** 2907 (1976).

[31] T. V. Long, A. W. Herlinger, E. F. Epstein, and I. Bernel, Inorg. Chem. **9,** 459 (1970).

[32] W. E. Estea, D. Y. Jeter, J. C. Hempel, and W. E. Hatfield, Inorg. Chem. **10,** 2074 (1971).